Efimov physics and the three-body parameter within a two-channel framework

P. K. Sørensen, D. V. Fedorov, A. S. Jensen, and N. T. Zinner
Department of Physics and Astronomy, Aarhus University, DK-8000 Aarhus C, Denmark
(Received 11 June 2012; revised manuscript received 18 July 2012; published 26 November 2012)

We calculate shallow three-body bound states in the universal regime, defined by Efimov, with inclusion of both scattering length and effective range parameters. We find corrections to the universal scaling laws for large binding energies. For narrow resonances we find a distinct nonmonotonic behavior of the threshold at which the lowest Efimov trimer merges with the three-body continuum. The origin of the three-body parameter is related to the two-body atom-atom interactions in a physically clear model. Our results demonstrate that experimental information from narrow Feshbach resonances and/or mixed systems are of vital importance to pin down the relation of two- and three-body physics in atomic systems.

DOI: 10.1103/PhysRevA.86.052516 PACS number(s): 31.15.ac, 67.85.−d, 03.65.Ge, 21.45.−v

I. INTRODUCTION

The counterintuitive behavior of three-body systems at the threshold for two-body binding is highlighted by the Efimov effect where an infinitude of geometrically scaling states appears [1]. While unsuccesfully sought for in nuclear physics [2], the effect has been confirmed and explored in ultracold atomic gases [3]. From the theoretical point of view these systems have been described accurately by universal theories that only take the lowest order scattering dynamics into account through the two-body scattering length, a [4,5]. However, the overall scale of the spectrum cannot be obtained in the universal theory, and the so-called three-body parameter, Λ, is needed to complete the formalism.

In ultracold atomic gases, trimer physics can be studied using interatomic Feshbach resonances [6] that provide tunability of a over many orders of magnitude. The parameters of these resonances in general will depend on the microscopic details of a particular atomic system. Still, in a surprising development, the Grimm group has reported strong indications that the three-body parameter is determined by the van der Waals length, $r_{\rm vdW}$ [7]. This implies that atomic trimer physics in the weakly bound limit only depends on two-body parameters. The experimental findings have generated a flurry of recent theoretical interest [8–11]. It has been suggested that the presence of many deep bound states in the two-body potential typical of alkali-metal atom systems will suppress the dependence on short-range physics due to a large inner repulsive barrier [9,10].

The most natural way to eliminate any need for a three-body parameter is to use a finite-range two-body potential that exhibits the known features of the interatomic interaction. Here we pursue this natural and straightforward approach to the issue of the origin of Λ in three-body physics. As three-body calculations with finite-range potentials are typically very cumbersome, it is highly desirable to have simple models that mimic the finite-range physics. Therefore we consider here a model with zero-range interactions that includes finite-range correction effects. Consequently, we solve the three-body Schrödinger equation using one- and two-channel models for the description of the Feshbach resonances that are used to control interactions in experiments [6]. The three-body parameter is considered parametrically in both models, and this allows us to study the threshold behavior of Efimov trimers as function of Λ and the width of the Fesbhach resonance, which is related to the effective range, r_e [6]. Here $r_{\rm vdW}$ and r_e are intimately connected through semiclassical calculations [12–14]. It is conceivable that this explains the observed values of Λ as r_e or $r_{\rm vdW}$ provides a background scale that determines the overall scale. However, given the delicate nonclassical nature of the universal trimer states, it is far from obvious if and how this can work out.

The experimental findings indicate that for several different atomic species the ratio of threshold scattering length $a^{(-)}$ for creation of Efimov trimers out of the three-body continuum is of order $a^{(-)}/r_{\rm vdW} = 8.5$–$9.5$ [9]. Here we show that this result can be obtained in a single-channel zero-range model for a specific choice of Λ, which can be related to the underlying two-body atom-atom physics in a natural way. Within a two-channel model we find an intriguing nontrivial behavior of $a^{(-)}$ for narrow resonances, *irrespective* of the three-body parameter; see Fig. 1. We also study the behavior of $a^{(-)}$ as a function of the number of bound states allowed by the two-body atomic potential for both one- and two-channel models. Generally, we find that the inclusion of effective range decreases $|a^{(-)}|$. Our results predict that narrow resonance systems are important for obtaining a full picture of the relation between two- and three-body parameters for universal bound-state physics.

II. METHOD

We consider a system of three identical bosonic particles using hyperspherical coordinates [19] defined from the Cartesian coordinates $\boldsymbol{r}_i,\boldsymbol{r}_j,\boldsymbol{r}_k$ through $\boldsymbol{x}_i = (\boldsymbol{r}_j - \boldsymbol{r}_k)/\sqrt{2}$ and $\boldsymbol{y}_i = \frac{2}{3}[\boldsymbol{r}_i - (\boldsymbol{r}_j + \boldsymbol{r}_k)/2]$ as hyper-radius, $\rho = \sqrt{\boldsymbol{x}_i^2 + \boldsymbol{y}_i^2}$, and hyperangle, $\alpha_i = \tan^{-1}\frac{|\boldsymbol{x}_i|}{|\boldsymbol{y}_i|}$. $\{i,j,k\}$ are cyclic permutations of $\{1,2,3\}$ and ρ is independent of this choice. We apply the hyperspherical adiabatic approach with wave function $\Psi(\rho,\Omega) = \rho^{-5/2}\sum_n f_n(\rho)\Phi_n(\rho,\Omega)$, where $\Omega = \{\alpha_i,\boldsymbol{x}_i/|\boldsymbol{x}_i|,\boldsymbol{y}_i/|\boldsymbol{y}_i|\}$ is a set of angular coordinates. We keep only the lowest adiabatic potential corresponding to $n = 0$, and index n is henceforth suppressed. For the description of Efimov trimer states, this approximation has proven extremely accurate [4]. The radial

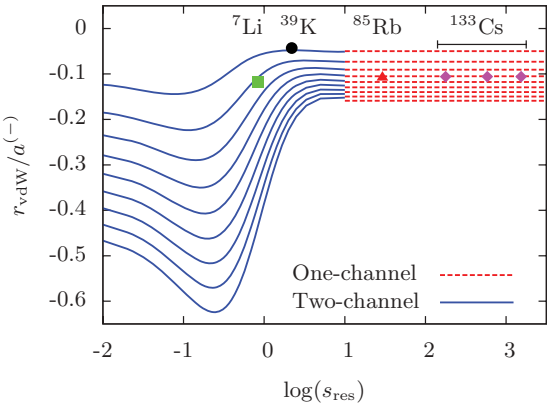

FIG. 1. (Color online) The threshold scattering length $a^{(-)}$ at which the lowest universal Efimov trimer merges with the three-atom continuum plotted against the strength, $s_{\rm res}$, of the Feshbach resonance. The right-hand side corresponds to broad resonances. The different curves of the linetypes show results with different three-body parameters, ρ_c, in units of the atomic van der Waals length, $r_{\rm vdW}$. The values of ρ_c decrease from top to bottom (precise values are given in the text). Experimental values are from ^{133}Cs [7,15], ^{7}Li [16], ^{39}K [17], and ^{85}Rb [18].

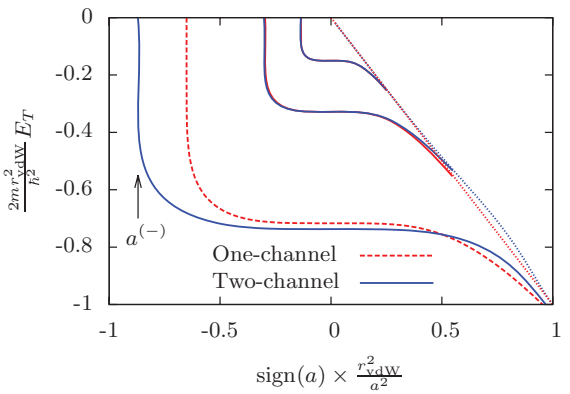

FIG. 2. (Color online) Trimer binding energy E_T vs scattering length a for the one- and two-channel models with effective range $r_e=-5r_{\rm vdW}$. $a^{(-)}$ is the threshold scattering length for the existence of the lowest trimer. Finely dotted lines indicate atom-dimer threshold for positive a. Successive states have a scaling of 515 [1] and for visibility the axes are scaled by the power 1/8.

equation is

$$\left(-\frac{d^2}{d\rho^2}+\frac{\lambda(\rho)+15/4}{\rho^2}-\frac{2mE}{\hbar^2}\right)f(\rho)=0, \qquad (1)$$

where $\lambda(\rho)$ is the eigenvalue to the hyperangular equation

$$\left(\tilde{\Lambda}^2+\frac{2m\rho^2}{\hbar^2}V\right)\Phi(\rho,\Omega)=\lambda(\rho)\Phi(\rho,\Omega), \qquad (2)$$

in which $\tilde{\Lambda}^2$ is the generalized angular momentum operator, V is the two-particle interaction potential, and m is the atomic mass. In Eq. (1), the nonadiabatic corrections are omitted as they are found to be negligible.

We use zero-range single-channel and a two-channel interaction models [20]. The former is accurate for broad Feshbach resonances (small r_e) and the latter for narrow resonances (large r_e). Both models contain the background scattering length in the open channel, $a_{\rm open}$. Our model must predict three-body properties solely from two-body potentials, so we must insist that $a_{\rm open}$ is a quantity most naturally associated to the two-body $r_{\rm vdW}$. In a semiclassical approach, the scattering length of such potentials is $\bar{a}\equiv 4\pi(\Gamma[1/4])^{-2}r_{\rm vdW}\approx 0.956 r_{\rm vdW}$ [12]. Then $a_{\rm open}$ should be identified with $r_{\rm vdW}$ to within a few percent. The resonance strength is related to r_e [20]. We characterize the strength by $s_{\rm res}=r_{\rm vdW}/|R_0|$, where R_0 is the effective range when $|a|=\infty$ [6].

Equation (1) is solved numerically for $f(\rho)$ with the condition $f(\rho_{\rm L})=0$ for large $\rho_{\rm L}$. At short distance the zero-range models used here require a cutoff, ρ_c, with $f(\rho_c)=0$ [4]. Initially, we consider ρ_c a parameter and study the three-body spectrum for different ρ_c and different $s_{\rm res}$. ρ_c is the coordinate-space equivalent of Λ. Below we relate the ρ_c to the two-body atomic potential.

III. RESULTS

In Fig. 2 we show trimer energies, E_T, as function of a for both one- and two-channel models. We find that the two-channel energies are generally lowest when $a<0$ and for $a>0$ the trimers cross before merging with the atom-dimer continuum. As indicated in Fig. 2, $a^{(-)}$ is the threshold scattering length for appearance of the lowest Efimov trimer on the negative a side. The two-channel model is here seen to move this threshold to the left, that is, to smaller negative $a^{(-)}$. These thresholds and the energy for $|a|=\infty$ are connected by universal relations, where lower energy on resonance translates to smaller $|a^{(-)}|$ at the threshold [1].

A systematic study of the influence of both ρ_c and r_e (or equivalently $s_{\rm res}$) is shown in Fig. 1, which is one of our main results. The values of $\rho_c/r_{\rm vdW}$ from top to bottom in Fig. 1 are 1.20, 0.82, 0.66, 0.58, 0.51, 0.47, 0.42, 0.40, and 0.38. They correspond to $n=0$ to 9 in Eq. (4) below. Both models agree for $s_{\rm res}\gg 1$, and we plot the two-channel model results only in the region where it deviates. We find that to reproduce the experimental data for $s_{\rm res}\gg 1$, a cutoff of $\rho_c/r_{\rm vdW}=0.58$ is required. However, for small $s_{\rm res}$, the same cutoff does not reproduce the known data point coming from ^{7}Li (other measurements have smaller $a^{(-)}$ [21,22], which is closer to our predictions). While we do find an increase toward the ^{39}K data point at small $s_{\rm res}$, it cannot be accommodated for the same ρ_c.

In general, we find that, irrespective of ρ_c, the inclusion of effective range brings a nonmonotonic behavior to $a^{(-)}$, and it tends to push the value of $a^{(-)}$ *down* for small $s_{\rm res}$ or large $|r_e|$. The reason can be seen in Fig. 3 where the adiabatic potentials for different effective ranges, $r_e/r_{\rm vdW}=0,-0.1,-1,-5$, are shown. At $r_e=0$ the bound states generally reside at large $\rho/r_{\rm vdW}$ [4]. The effective range causes an additional repulsive barrier, initially leading to less bound energies when $|r_e|$ is small, since the bound state sitting at large ρ will feel the barrier at first. When the effective range increases the attractive region will ultimately lead to an increase in bound-state energy as the wave function starts to occupy the pocket at smaller ρ.

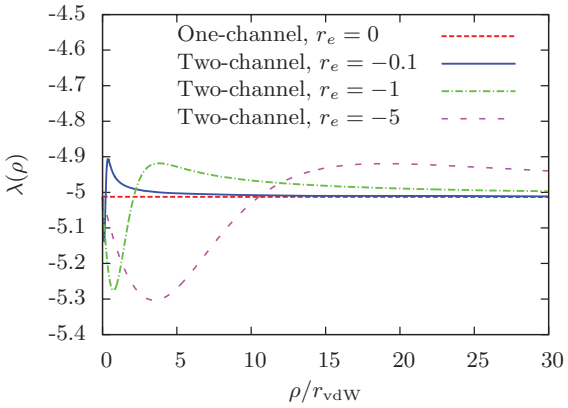

FIG. 3. (Color online) The lowest adiabatic potentials multiplied by ρ^2 as functions of hyper-radius, ρ, for the zero-range one-channel model and three different effective ranges for the two-channel model.

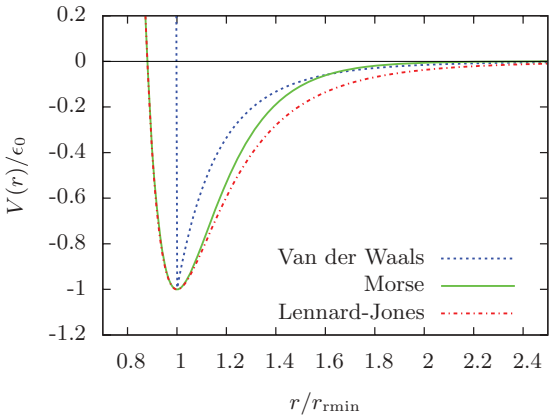

FIG. 4. (Color online) Typical two-body neutral atom-atom potentials, including the hardcore van der Waals potential of Eq. (3), the Lennard-Jones potential, $V_{\rm LJ}(r) = \frac{C_{10}}{r^{10}} - \frac{C_6}{r^6}$, and the Morse potential, $V_M(r) = 4\epsilon_0(e^{-2\alpha(r-r_0)} - e^{-\alpha(r-r_0)})$. Here C_6, C_{10}, and α are parameters. They have all been fitted to have the same overall energy, ϵ_0, at the radius of the potential minimum, $r_{\rm min}$.

This is in sharp contrast to the study in Ref. [11], which finds the opposite behavior. As argued above, it is physically reasonable since E_T is lower at finite $r_e < 0$. We notice that our two-channel model has $r_e < 0$, which is consistent with the usual theory of Feshbach resonances [6]. Reference [11] appears to accommodate also $r_e > 0$ and this may resolve the discrepancy.

IV. CONNECTION TO TWO-BODY POTENTIAL

The zero-range model studied above does not carry information about the van der Waals length as it stands. However, the three-body parameter or cutoff, ρ_c, has a physical meaning as it provides a hard-core repulsion in hyperspherical three-body coordinates. To connect the formalism to experimental data, it is therefore necessary to find a relation between the two-body atomic physics and ρ_c. Below we consider different two-body interaction models and derive analytical formulas for the behavior of $a^{(-)}$ as the two-body interaction parameters are varied.

In Fig. 4 we plot Morse, Lennard-Jones, and a van der Waals potential with a hard-core at r_c. We first focus on the van der Waals plus hard-core model,

$$V(r) = -\frac{C_6}{r^6}, \quad r > r_c \tag{3}$$

where $r_{\rm vdW} = (\frac{mC_6}{\hbar^2})^{1/4}$. In order to relate the behavior of this potential to the physics of a Feshbach resonance, we use the formula [12,14] $a = \bar{a}(1 - \tan\Phi)$ with $\Phi = \frac{2r_{\rm vdW}^2}{r_c^2} - \frac{3\pi}{8}$, where a diverges when $\Phi = (n + \frac{1}{2})\pi$ for integer n, which counts the number of s-wave bound states accommodated by the potential. Thus

$$n = \frac{2}{\pi}\left(\frac{r_{\rm vdW}}{r_c}\right)^2 - \frac{7}{8} \tag{4}$$

rounded to highest nearby integer.

In the zero-range single-channel model ρ_c and $a^{(-)}$ are related, since ρ_c is the only length scale available. However, it is a nontrivial matter to determine this relation within the model. Numerically, we find the linear relation $a^{(-)} = -\delta\,\rho_c$, with $\delta = 31.756$. To cast this relation into a form that depends only on two-body physics, we observe that the two-body hard core at r_c is also responsible for a three-body hard-core cutoff, more precisely $\rho_c = \sqrt{2}r_c$. This condition ensures that when each two-body subsystem has radius $r \geqslant r_c$, the third particle will also be outside r_c with respect to the others (see Ref. [23] and the supplementary note A). We note that this relation is not the same as the ρ_c used in Ref. [9]. Using $a^{(-)} = -\delta\,\rho_c$ we obtain

$$\frac{a^{(-)}}{r_{\rm vdW}} = -\frac{2\delta}{\sqrt{(n + \frac{7}{8})\pi}}. \tag{5}$$

This semianalytical expression for the threshold in terms of the number of bound states is one of our main results.

The relation in Eq. (5) is plotted in Fig. 5 along with the experimental data and the numerical results obtained from the two-channel model for different value of $s_{\rm res}$. The one-channel model is consistent with data for $n \sim$ 10–20 and fits the universal ratio of Ref. [9] for $n = 13$. This is also consistent

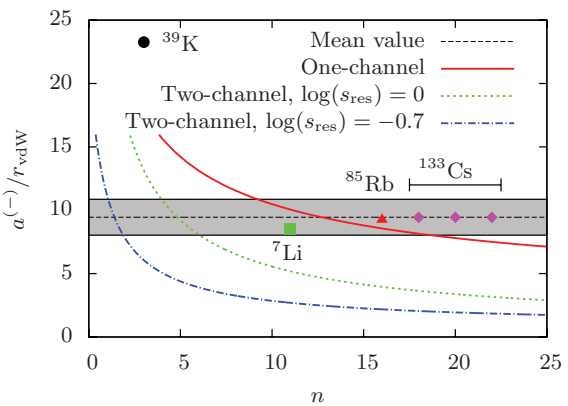

FIG. 5. (Color online) Semianalytic results for $a^{(-)}$ plotted against number of bound states in the two-body van der Waals plus hard-core potential. The horizontal position of the experimental data is arbitrary. The grey band indicates the 15% margin around the mean value of ~9.8.

TABLE I. Potential parameters, R_e (bond length) and D_e (dissociation energy) [24], and estimated number of bound states for Lennard-Jones, $n_{\rm LJ}$, and Morse, n_M, potentials.

	Li	K	Rb	Cs
R_e (Å)	2.67	3.92	4.18	4.65
D_e (eV)	1.06	0.52	0.49	0.45
$n_{\rm LJ}$	41	99	152	201
n_M	28	67	103	137

with the findings of Ref. [10], although the data only go to $n = 10$. Actually, the $n^{-1/2}$ behavior that we find here seems to also appear in Ref. [10], where an extension to higher n could confirm this prediction.

Even more interestingly, our results for small $s_{\rm res}$ indicate that $|a^{(-)}|$ drops faster with n than for $s_{\rm res} \gg 1$. This is seen in the experimental data on ^{7}Li, which is slightly below the ^{85}Rb and ^{133}Cs points, but our model seems to overestimate this trend. Clearly, more results on narrow resonance systems are required to address the question of effective range corrections. We expect a lower $|a^{(-)}|$ value than for broad resonances.

V. TWO-BODY POTENTIAL MODELS

Above we employed a van der Waals plus hard-core potential. However, as seen in Fig. 4, more realistic Lennard-Jones or Morse potentials have a smooth behavior of the inner barrier. This implies only minor quantitative corrections that nevertheless deserve to be addressed along with the number of bound states expected in a real alkali-metal dimer.

The number of s-wave bound states in the Lennard-Jones (LJ) and Morse (M) potentials can be estimated analytically and yields [25] $n_{\rm LJ} = 0.361\sqrt{\beta} - \frac{5}{8}$ and $n_M = 0.245\sqrt{\beta} - \frac{1}{2}$, where $\beta = \frac{m r_{\rm min}^2 \epsilon_0}{2\hbar^2}$ with $r_{\rm min}$ the radius at which the potential takes its minimal value, ϵ_0. For comparison, the expression in Eq. (4) can be written $n = 0.225\sqrt{\beta} - \frac{7}{8}$, with $r_{\rm min} \leftrightarrow r_c$ in β. The similarity of these expressions makes it clear that the behavior seen in Fig. 5 is generic and does not depend on our choice of two-body potential. The difference in constant provides only a minor quantitative change in the numbers.

An important question, however, remains about the number of bound states in a real alkali-metal dimer system. Using the molecular dissociation energy, $\epsilon_0 = D_e$, and the bond length, $r_{\rm min} = R_e$, of Ref. [24], we list the numbers for Li, K, Rb, and Cs dimers in Table I. The estimated number of bound states is outside the axis in Fig. 5 and also much beyond the results shown in Ref. [10]. The agreement with theory at a rather limited number of bound states ($n \sim 10$–20) is then quite surprising.

A number of important observations can be made. First, the decrease of $|a^{(-)}|$ with n is weak, and a shift of the length scale in Fig. 5 would therefore place the one-channel model within the experimental range for larger n and it would stay within the 15% deviation from the mean for a larger interval (since the slope at larger n decreases even faster). Second, the experimental data might indicate that only a certain number of bound states play an active role. Equivalently, even if the two-body potential is very deep, only the upper part of the two-body potential and the bound states closest to threshold set the scale of the three-body problem. This appears to be very reasonable since we are considering universal Efimov trimers here and not strongly bound three-body states. Third, the case of small $s_{\rm res}$ has $|a^{(-)}| \propto n^{-r}$ with $r > 1/2$ as seen in Fig. 5. This implies that narrow resonance systems should be even more insensitive to n beyond a certain lower limit.

We can give a quantitative argument for the lack of sensitivity to the many deeper bound states in a van der Waals potential. The number of bound states, $n(E)$, as a function of energy, E, counted from the $E = 0$ threshold and down within the JWKB (the semiclassical approximation of Jeffreys, Wentzel, Kramers, and Brillouin) approximation is $n(E) = n_0(|E|/E_{\rm vdW})^{1/3}$, where n_0 is the total number (given in Table I for different potentials) and $E_{\rm vdW} = \hbar^2/m r_{\rm vdW}^2 > 0$ is the depth of the potential [26]. For the $s_{\rm res} \gg 1$ cases (^{85}Rb and ^{133}Cs), $n(E)/n_0 \sim 0.10$–0.20, which implies $|E|/E_{\rm vdW} \sim 0.001$–$0.01$. Numerically we find a three-body energy on resonance $E_3 = 0.006 E_{\rm vdW}$ (using $\rho_c = 0.58 r_{\rm vdW}$). However, universality relates $E_3 = \hbar^2\kappa^2/m$ and $a^{(-)}\kappa \sim -1.51$ [1,5]. The energy scale at the continuum threshold is given by $a^{(-)}$ through $|E| \sim \hbar^2/m(a^{(-)})^2 = 0.003 E_{\rm vdW}$, in agreement with the interval above. In the case of ^{7}Li, E_3 is similar but this is compensated by a smaller n_0 so this case can also be explained. For heavier alkali atoms with narrow resonance, our two-channel results predict a smaller $a^{(-)}/r_{\rm vdW}$ than 9.8, which is a good experimental test of our theory.

VI. CONCLUSIONS

We derive an analytical formula that connects $a^{(-)}$ and the number of s-wave bound states, n, in the two-body potential, which agrees with recent experiments $n \sim 10$–20. While alkali atoms typically have larger n, we argue quantitatively that only a subset determine the properties of Efimov three-body states. We find nonmonotonic behavior of $a^{(-)}$ with increasing effective range, which demonstrates that systems with narrow Feshbach resonances will provide both qualitative and quantitative understanding of universality and the origin of the three-body parameter. This means that different atomic species that typically have narrow resonances and a denser spectrum would be very helpful.

ACKNOWLEDGMENTS

We thank Chris Greene, Georg Bruun, and Frank Jensen for useful discussions. This work is supported by the Danish Council for Independent Research–Natural Sciences (DFF-FNU).

APPENDIX: DETERMINATION OF THE HYPER-RADIAL BOUNDARY CONDITION

The atom-atom two-body potential has a steep repulsive inner core, which we assume for the moment can be represented by a hard wall, that is, an infinite potential for radii $r < r_c$. In this case the boundary condition is simply that the two-body wave function must be zero at r_c. This must then be translated in the three-body problem, where it implies that the total wave function must be zero whenever any of the relative distances between two out of the three atoms is less than or equal to r_c.

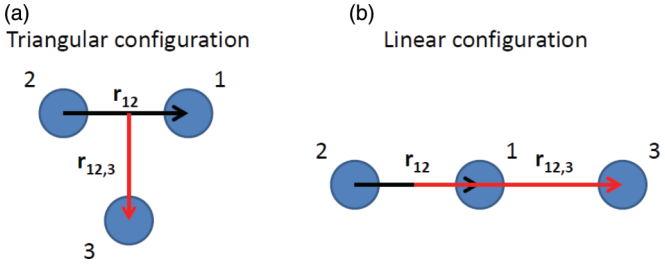

FIG. 6. (Color online) Schematic of the (a) triangular and (b) linear configurations for an equal mass three-body system. $\boldsymbol{r}_{12}$ and $\boldsymbol{r}_{12,3}$ indicate the two Jacobi relative vectors.

Any penetration of the wave function into the wall would cost an infinite amount of energy and is thus forbidden.

A neat and elegant way to obtain a condition on ρ is the following. As is easily shown, the hyper-radius fulfills

$$\rho^2 = \frac{1}{3}\sum_{i<k}(\boldsymbol{r}_i - \boldsymbol{r}_k)^2 = \frac{1}{2}\boldsymbol{r}_{12}^2 + \frac{1}{3}\boldsymbol{r}_{12,3}^2, \qquad \text{(A1)}$$

where $\boldsymbol{r}_{12} = \boldsymbol{r}_1 - \boldsymbol{r}_2$ and $\boldsymbol{r}_{12,3} = \boldsymbol{r}_3 - (\boldsymbol{r}_1 + \boldsymbol{r}_2)/2$ are respectively the relative vector from particles 2 to 1 and the relative vector from the center of mass of 1 and 2 to particle 3 (see Fig. 6).

Now consider the triangular configuration shown in Fig. 6(a). From the formula in Eq. (A1), it is clear that when $r_{12} = r_c$ this setup also has $\rho = r_c$. However, the linear configuration in Fig. 6(b) with $\rho = r_c$ will then have two atoms that are within the hard-core radius and yield an infinite contribution to the potential energy (this happens, for example, when $|\boldsymbol{x}| = r_c$ and $\boldsymbol{y} = 0$, putting atom 3 midway between 1 and 2).

Consider instead the linear configuration with $r_{12} = r_c$ and impose the requirement $r_{23} \geqslant r_c$, where $\boldsymbol{r}_{23} = \boldsymbol{r}_2 - \boldsymbol{r}_3$. Since we have $\boldsymbol{r}_{12,3} = \boldsymbol{r}_{23} + \boldsymbol{r}_{12}/2$ we get

$$\rho^2 \geqslant r_c^2\left(\tfrac{1}{2} + \tfrac{2}{3}\left[1 + \tfrac{1}{2}\right]^2\right) = 2r_c^2. \qquad \text{(A2)}$$

We thus see that the condition $\rho > \sqrt{2}r_c$ ensures that both triangular and linear configurations are outside the hard-core regions. Since these configurations are extremal, the condition implies that no regions with infinite potential are sampled by the hyper-radial three-body wave function.

The rigourous formal argument for the validity of the relation $\rho_c = \sqrt{2}r_c$ using the hyperspherical approach can be found in Ref. [23], where the relation is derived using a square well potential. The asymptotic region is precisely $\rho > \sqrt{2}r_c$ as found above. Here we assumed a hard-core potential for simplicity, which gives the factor of $\sqrt{2}$. For a real atom-atom potential, the hard core is slightly softer (typically of the $1/r^{12}$), which may lead to a minor change in the factor.

The hyperspherical approach and the use of the lowest hyper-radial potential to describe Efimov states is a well-known and accurate procedure. Additionally, as we have shown above, a hard-core repulsion in the two-body potential naturally generates a hyperspherical cutoff radius, $\rho_c = \sqrt{2}r_c$. This constitutes a clear and simple explanation of the repulsive core found in the numerical calculations in Ref. [10], and our results demonstrate that a simple model can accurately describe those numerically involved findings. We thus see how the value $\sqrt{2}r_c$ for the three-body cutoff parameter naturally derives from the hard-core behavior of the corresponding two-body potential.

[1] V. N. Efimov, Sov. J. Nucl. Phys. **12**(5), 589 (1971).
[2] A. S. Jensen, K. Riisager, D. V. Fedorov, and E. Garrido, Rev. Mod. Phys. **76**, 215 (2004).
[3] F. Ferlaino and R. Grimm, Physics **3**, 9 (2010).
[4] E. Nielsen, D. V. Fedorov, A. S. Jensen, and E. Garrido, Phys. Rep. **347**, 373 (2001).
[5] E. Braaten and H. W. Hammer, Phys. Rep. **428**, 259 (2006).
[6] C. Chin, R. Grimm, P. S. Julienne, and E. Tiesinga, Rev. Mod. Phys. **82**, 1225 (2010).
[7] M. Berninger, A. Zenesini, B. Huang, W. Harm, H. C. Nagerl, F. Ferlaino, R. Grimm, P. S. Julienne, and J. M. Hutson, Phys. Rev. Lett. **107**, 120401 (2011).
[8] P. Naidon, E. Hiyama, and M. Ueda, Phys. Rev. A **86**, 012502 (2012).
[9] C. Chin, arXiv:1111.1484v2.
[10] J. Wang, J. P. D'Incao, B. D. Esry, and C. H. Greene, Phys. Rev. Lett. **108**, 263001 (2012).
[11] R. Schmidt, S. P. Nath, and W. Zwerger, arXiv:1201.4310v2.
[12] G. F. Gribakin and V. V. Flambaum, Phys. Rev. A **48**, 546 (1993).
[13] B. Gao, Phys. Rev. A **58**, 4222 (1998).
[14] V. V. Flambaum, G. F. Gribakin, and C. Harabati, Phys. Rev. A **59**, 1998 (1999).
[15] T. Kraemer *et al.*, Nature (London) **440**, 315 (2006).
[16] S. E. Pollack, D. Dries, and R. G. Hulet, Science **326**, 1683 (2009).
[17] M. Zaccanti *et al.*, Nat. Phys. **5**, 586 (2009).
[18] R. J. Wild, P. Makotyn, J. M. Pino, E. A. Cornell, and D. S. Jin, Phys. Rev. Lett. **108**, 145305 (2012).
[19] Y. Suzuki and K. Varga, *Stochastic Variational Approach to Quantum-Mechanical Few-Body Problems* (Springer-Verlag, Berlin, 1998).
[20] P. K. Sørensen, D. V. Fedorov, and A. S. Jensen, Few-Body Syst. (2012), doi: 10.1007/s00601-012-0312-7.
[21] N. Gross, Z. Shotan, S. Kokkelmans, and L. Khaykovich, Phys. Rev. Lett. **103**, 163202 (2009).
[22] N. Gross, Z. Shotan, S. Kokkelmans, and L. Khaykovich, Phys. Rev. Lett. **105**, 103203 (2010).
[23] A. S. Jensen, E. Garrido, and D. V. Fedorov, Few-Body Syst. **22**, 193 (1997).
[24] G. Igel-Mann, U. Wedig, P. Fuentealba, and H. Stoll, J. Chem. Phys. **84**, 5007 (1986).
[25] G. D. Mahan and M. Lapp, Phys. Rev. **179**, 1 (1969).
[26] The number of bound states, $n(E)$, can be found within the WKB formalism by considering the integral $\int_{r_i}^{r_o}\sqrt{E - V(r)}dr = \pi\hbar[n(E) + 1/4]$, which is a measure of the number of nodes in the wave function with energy $E < 0$. Using $E = 0$ one obtains the total number, n_0. The van der Waals potential does not yield analytical results, but we numerically find that $n(E) \propto E^{1/3}$, which when normalized yields the relation in the text.